9B.2 Collision-induced drop oscillations from wind-tunnel experiments

Merhala Thurai[1], Miklos Szakall[2], V. N. Bringi[1], and S. K. Mitra[2]

[1]Colorado State Univ., Fort Collins, CO
[2]Johannes Gutenberg University, Mainz, Germany

1. Introduction

Knowledge of drop shapes and drop oscillations is of central importance for deriving retrieval algorithms for drop size distribution (DSD) parameters and rain rate as well as for attenuation-correction at higher frequencies (C, X-bands) from polarimetric radar (e.g., Bringi and Chandrasekar 2001 and references contained therein). Earlier work using 2D video disdrometer (2DVD) measurements of drop shapes (Thurai et al. 2007) for drop diameters larger than 2 mm had lead to the derivation of the most-probable shapes as well as the shape variations due to drop oscillations. The 2DVD-based shapes had also been shown to be in good agreement with wind-tunnel measurements for D > 2 mm (Thurai et al., 2009). Moreover, a thorough examination of the 2DVD camera data in natural rain from several locations have shown that in the vast majority of cases, the most 'probable' shapes conform to those arising primarily from the axisymmetric (2,0) oscillation mode (Beard et al. 2010). The other two oscillation modes, namely, mode (2,1) and mode (2,2), did not seem to be contributing to the probable shapes. Fig. 1 shows the most probable shapes for drop equivalent diameters of 3 and 4 mm from the 2DVD measurements in natural rain and fig. 2 shows the three oscillation modes at the various oscillation cycles. A large drop size is used to depict the three modes clearly.

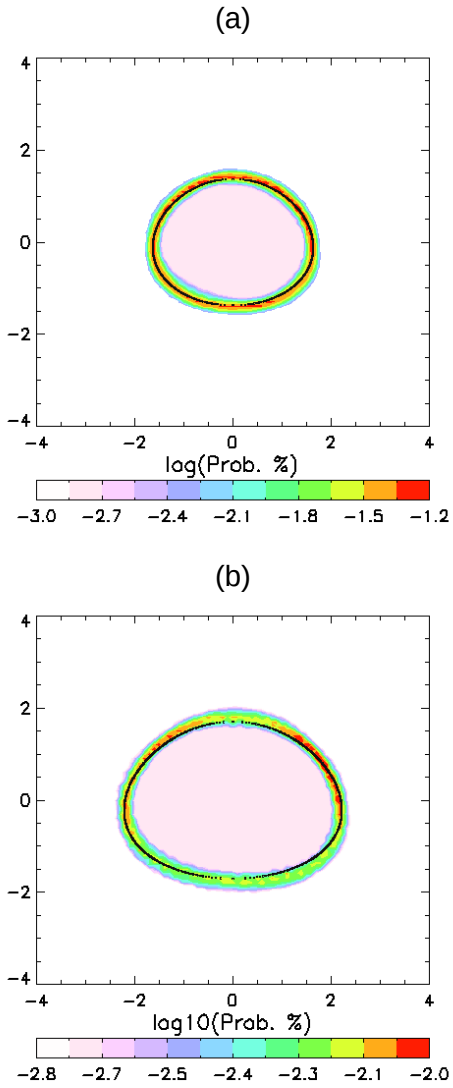

Fig. 1: Drop shape measurements in natural rain from 2DVD for drop diameters of (a) 3 - 3.25 mm, and (b) 4 – 4.25 mm. For (a), the number of drops used is 9300 and for (b) 904. X and Y dimensions are in mm. The black line represents the most probable shapes from the 80 m fall experiment.

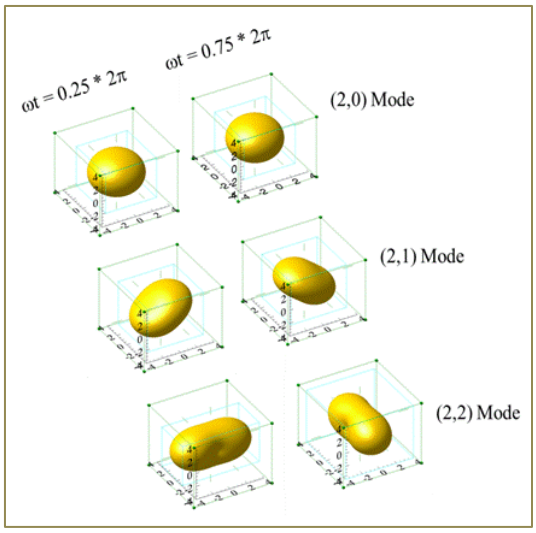

Fig. 2: Three-dimensional views of the three oscillation modes, for two phases of the oscillation cycle: (i) $\omega t = \frac{1}{4} * 2\pi$ and (ii) $\omega t = \frac{3}{4} * 2\pi$. Equations in Beard and Kubesh (1991) have been used to generate these figures, for D=6 mm and 10% oscillation amplitude.

There have been a few exceptions, however. A recent study (Thurai et al., 2013) of an intense organized line convection using two collocated 2D video disdrometers (2DVD) and a C-band polarimetric radar, it was possible to infer the occurrence of mixed mode drop oscillations, probably sustained by collisional forcing. Additionally, the mixed mode oscillations seemed to be coupled with reduced fall velocities for moderate-to-large sized drops. These inferences were based on the fact that (a) a significant fraction of the larger drops (e.g. drop diameters of 3 mm and larger) from the 2DVD measurements did not possess rotational symmetry – when the line convection had passed over the 2DVD location - and (b) that the fall velocity distributions showed a negative skewness towards lower values. Polarimetric radar information such as ρ_{hv} had also supported the notion of mixed mode oscillations because of their lower values than those expected from equilibrium shapes (together with the wide DSDs measured during the passage of the line).

To investigate collision-induced drop oscillations, we have conducted experiments using the vertical wind-tunnel facility, based in Mainz, Germany. In this paper, we briefly describe the experiments, and present the results, followed by a discussion, particularly in conjunction with the 2DVD measurements during the aforementioned rain event.

2. Wind-tunnel measurements

The laboratory study on drop oscillations was carried out at the vertical wind tunnel facility at the University of Mainz (Pruppacher 1988; Mitra et al. 1992), where drops and other hydrometeors can be freely suspended individually at their terminal velocities in a vertical airstream. Wind tunnel speed, temperature, and humidity of the tunnel air are controlled and continuously recorded. Wind-tunnel speeds up to 40 m s^{-1} are possible so that water drops of all sizes between 40 μm and 8 mm can be investigated. Note that drop shapes are not expected to change appreciably with moderate temperature and pressure differences (see Beard 1976).

The airstream in the tunnel is laminar with a residual turbulence level below 0.5%. For vertical air speeds typical for millimeter-size drop measurements the tunnel has a uniform velocity distribution around the whole cross-sectional area up to the boundary layer (Vohl 1989). This ensures that the water drops are floating in a stable fashion for relatively long time periods (from a few hundred milliseconds up to a few minutes depending on the size) within the tunnel.

The oscillation of the floating raindrops was continuously recorded by a high-speed digital video camera (Motion-Pro

X; Redlake, Inc.). The complementary metal oxide semiconductor (CMOS) chip of the camera ensured 1000 frames per second (fps) recording speed at maximum resolution of 1280 × 1024 pixels, and 2000 fps at half-resolution of 1280 × 512 pixels. The measurements were carried out by attaching an objective with a magnification of 1:2 to the camera. The pixel size of the camera chip is 12 μm; thus, a spatial pixel resolution of 24 μm was obtained. In the measurements, a diffuse background illumination was maintained by a milk-glass plate illuminated by a 400-W dc cold light lamp.

The oscillation frequency, as well as the mathematical mean and the amplitude of the axis ratio of the drops, was determined by processing the recorded 8-bit images individually. A computer program written in the LabView programming language was developed to carry out the image processing and to determine the width and the height and, consequently, the axis ratio of the drops as a function of time. From the time series of the axis ratio, one could determine the oscillation frequency and the (mathematical) mean axis ratio. The detailed calculation of the measurement error regarding the oscillation frequency and the axis ratio can be found in Szakáll et al. (2009). Briefly, the oscillation frequency can be measured with an error of 0.21 Hz for a water drop of 4.8 mm in diameter, while a relative error of less than 2% is estimated for the axis ratio determination.

3. Analysis methods

A novel method was developed to identify and distinguish the axisymmetric (2,0), transverse (2,1) and horizontal (2,2) oscillation modes of freely floating raindrops. First the recorded grey level images of the oscillating raindrops were transformed to black-and-white (BW) images. Afterwards, the individual images were further analysed with the following three algorithms in order to identify the existence of the (2,0), (2,1) and (2,2) oscillation modes.

The axis ratios of the drops were determined by calculating the ratio of the largest vertical and horizontal chord of the drop. The temporal variation of the axis ratio, i.e. the continuously varying oblate-prolate deformation, is primarily caused by the axisymmetric (2,0) oscillation mode. However, the other two modes also contribute to the axis ratio variation, so that in the temporal variation of the axis ratio beating can be observed. As the other two modes normally correspond to lower amplitudes and frequencies, the (2,0) mode is the primary carrier mode in the beating. Its frequency can be identified as the highest peak of the frequency spectrum of the axis ratio variation.

The frequency of the (2,1) transverse oscillation mode can eventually also be determined from the frequency analysis of the axis ratio variation. This procedure requires, however, that the frequency resolution of the measurement is high enough to be able to distinguish between the (2,0) and (2,1) frequencies. In other words, the observation time should exceed the time period of beating resulted by the oscillation modes. This requirement can be fulfilled if the drops are levitating in the field of view of the camera for time periods of a few seconds which is essentially rare. If a drop would oscillate exclusively in the (2,1) mode (which has never been observed in our wind tunnel measurements), its shape would be changed in a way like the drop as a whole would be canted around a horizontal axis. The maximum of this apparent canting is only a few degrees. The canting angle variations of the oscillating drops in the present experiments were determined as

follows: First, a horizontally oriented rectangle was fitted to the drop image and the axis ratio of the rectangle was calculated. Next, the BW image was rotated by 1°, and the former process was repeated. By rotating the BW image to 180° in 1° steps and calculating the corresponding axis ratios of the best-fit rectangles, the orientation of the one with the minimum axis ratio gave the "apparent canting angle" of the drop. Repeating this algorithm for all images, the "apparent canting angle" variation of the drop during oscillation was determined. The frequency of the (2,1) mode was obtained by frequency analyzing the temporal variation of the "apparent canting angle".

The frequency of the (2,2) horizontal mode of an oscillating raindrop was determined from the temporal variation of its projected area. First the volume equivalent diameters were determined from the BW images using the integration method as follows. In the recorded digital images the drops were composed of 1-pixel thick horizontal slices. Hence, the volume of the drop could be determined as the sum of the volumes of discs with a thickness of one pixel and with a diameter equal to the width of one slice.

Since a drop oscillating in the (2,2) mode is not rotationally symmetric around the vertical axis at any phase, the volume calculated from the side projected area of the drop, i.e. not the true drop volume but a pseudo volume assuming vertical axis-symmetry, is not constant during the oscillation. Hence, a periodic change in the calculated drop volume could be observed. The other fundamental oscillation modes, i.e. the (2,0) and the (2,1) do not contribute to the variation of the calculated drop diameter, so that the frequency of the (2,2) mode could exclusively be determined from the frequency analysis of the periodic change of the calculated drop volume.

Figure 3 shows results of the above described algorithms for identifying the different oscillation modes in case of a 4.6 mm diameter water drop freely floating in the vertical wind tunnel. The time series and the corresponding frequency spectra of the axis ratio (a and b), the canting angle (c and d), and the volume-equivalent drop diameter (e and f) are presented. The arrows and the numbers indicate the frequencies computed using the equations in Feng and Beard (1991).

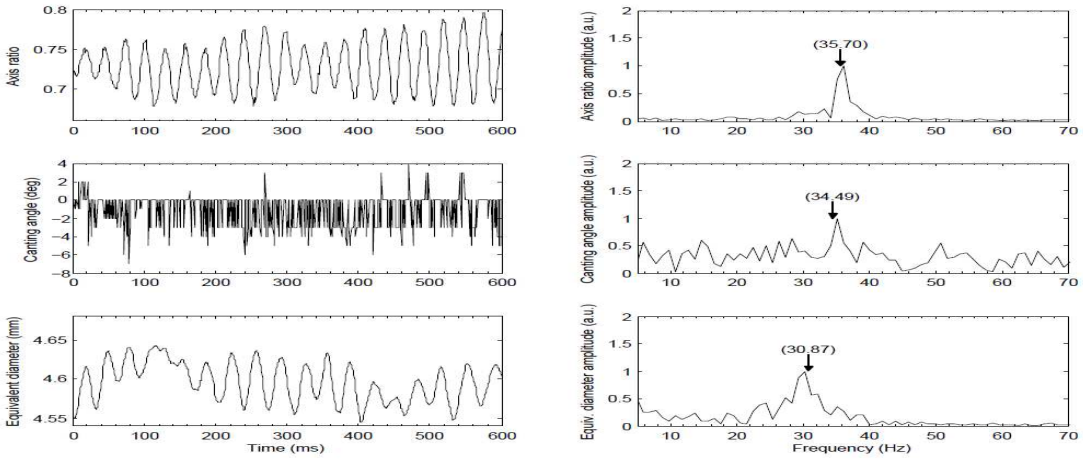

Figure. 3: Variation of of axis ratio, 'apparent' titl angle and the 'apparent' volume with time (left panels) and their frequency components to identify the different modes.

4. Collision experiments

More than 200 collision experiments were carried in the Mainz vertical wind tunnel, from which 130 were recorded with a high speed digital video camera. Many of the recorded collision events had to be abandoned because the drops were not in the focal plane of the camera. Finally, we were able to analyze around 40 collision events; among them were 27 which ended with coalescence and the remaining with non-coalescence collision.

The sizes of the colliding drop pairs were chosen to be typical for real-atmospheric conditions, i.e. for the collector drops, they were in the 2.4 mm - 3 mm drop diameter range, while the small droplets had sizes of around 500 microns. In each case, the collector drop was freely-floated inside the wind-tunnel until a small droplet (injected from below) coming from the upstream side of the larger drop collided with it. It turned out from the post-analysis of the experiments that the small droplet did not reach their terminal velocities at the moment of collision because the distance from the injection point of the droplets to the place where the collision took place was not sufficient to accelerate to their terminal speed. As a consequence, the collision kinetic energy (CKE) was also lower than the values would be in the free atmosphere. The range of the CKE in the present experiments (from 0.18 to 1 μJ), however, overlapped on the theoretical CKE range (from 0.35 to 2 μJ) corresponding to drops falling at terminal speeds.

(a) Coalescence

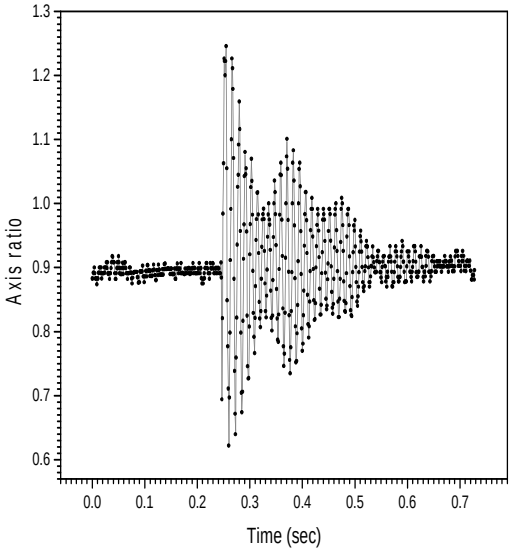

(b) No coalescence

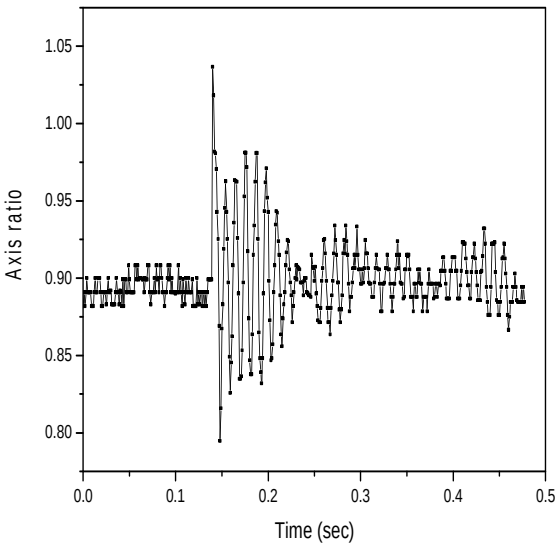

Fig. 4: Axis ratio variation with time (sec) before, during and after collision

A typical example of the axis ratio variation of a drop during a collision-coalescence process is presented in Figure 4a. The collector drop was freely floating in the wind tunnel until a small droplet coming from the upstream side of the drop collided with it at 250 milliseconds. The time moment of the collision is coupled with a large axis ratio variation. The multimode oscillation of the drops is obvious from the beating in the time series. Around 450 milliseconds after collision the perturbation caused by the collision is effectively damped out and the drop is oscillating with the same amplitude as before collision.

Figure 4b represents the time evolution of the axis ratio during a collision of two drops where no coalescence occurred. In this case the axis ratio variation is not so pronounced as in the former case but beating can again be recognized.

5. Data analysis

The frequency spectra of the oscillations of drops before (left panels) and after the collision processes (right panels) are shown in Figure 5. In both the coalescing and non-coalescing cases the (2,0) mode is the most pronounced oscillation mode before collision (plotted as black line). The (2,2) mode (red line, calculated from the virtual volume variation as described above) is also active in both cases though its amplitude is very low. The (2,1) mode which is plotted as green line is not present before collision.

After collision the (2,1) mode, which is given by the green line and calculated from the apparent tilting angle of the drop, becomes active, and actually it becomes the dominating oscillation mode, i.e. the mode which determines the axis ratio variation. The axis ratio after collision was increased by 0.9% in case of coalescence and by 0.44% in cases of breakup, as a consequence of the dominance of the (2,1) mode. Furthermore, in the coalescing case the amplitude of the (2,2) mode is also significantly large and appears in the frequency spectrum of the axis ratio variation, and seemingly in the spectrum of the tilting angle variation. The small deviation of the peak frequencies in the (2,0) and (2,1) spectra from the peak of the (2,2) mode (at 78 Hz) is most probably a result of the applied frequency analysis (discrete time Fourier-transformation).

The oscillation modes in the non-coalescing case are not so pronounced as in the coalescing case. This results in noisier frequency spectra. In spite of it, the existence of the (2,0), (2,1) and (2,2) modes is obvious, though the origin of the large secondary peaks appearing in the spectra has to be further analyzed.

6. Discussion

Data analysis clearly shows that the larger drop - upon collision - undergoes mixed-mode oscillations, with (2,1) and (2,2) modes dramatically increasing in oscillation amplitudes. The perturbation caused by the collision is seen to last for over several hundred milliseconds before effectively getting damped out and reverting to its usual (2,0) oscillation mode as the dominant mode. The coalescence cases show somewhat more pronounced mixed mode oscillations compared with the non-coalescence cases. Note, the decay time constant is considerably larger than those used by Johnson and Beard (1984) collision model.

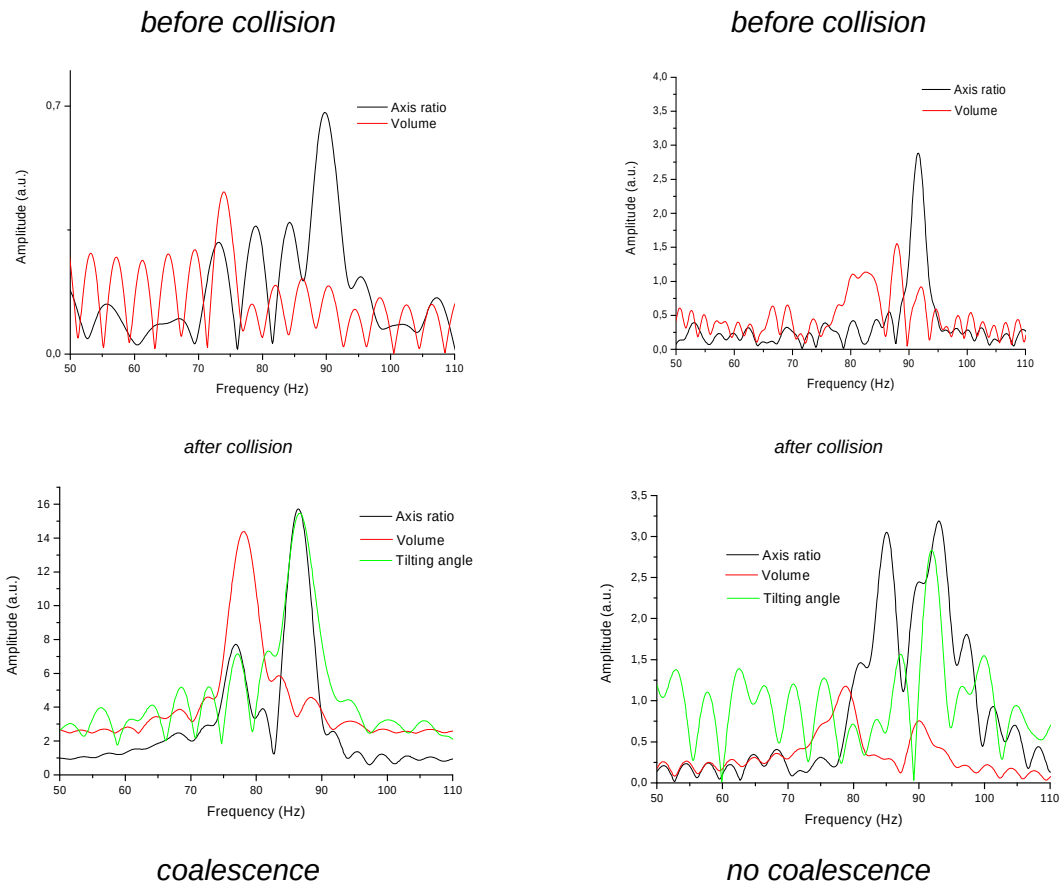

Figure 5: Oscillation amplitudes before and after collisions

The fact that the damping time constant for the mixed mode oscillations to decay is of the order of several hundred milliseconds must mean that if in real-atmospheric conditions the collision frequency has similar time constant, then sustained drop collisions can cause significant fraction of the drops at any instant in time to be in mixed mode oscillation state (and not have rotational axis symmetry). Referring back to the event analyzed in Thurai et al. (2013) using 2DVD data and the C-band ARMOR observations in Huntsville, Alabama, the most probable explanation is that drops are undergoing mixed mode oscillations within the line convection region, and that these are probably due to drop collisions, e.g. 3 mm with tiny drops (probable scenario according to literature). If such collisions occur typically at a rate of 0.2 s^{-1} (for 3 mm drops in a 55 dBZ reflectivity rain column, from Rogers, 1989), then it is conceivable that collisions can sustain drop oscillations (against viscous dissipation) for a significant fraction of the 3 mm drops. This has also been hypothesized in Jameson and Durden (1996) from airborne measurements of copolar and cross-polar backscatter from tropical storms. For the event discussed in Thurai et al. (2013), high rain intensity confined within the narrow line convection would significantly increases the likelihood of drop collisions. Moreover, in the case of rain clustering (see for example Jameson and Kostinski, 1999) which may well be the case within the embedded line convection in that event, drop collision rates can increase significantly by a

significant factor (McFarquhar, 2004). The methodology described in Tokay and Beard (1996) can be used to assess the importance of collisional-forcing of drop oscillations relative to intrinsic aerodynamic mechanisms (which for larger drops is dominated by the axisymmetric mode). The main input to the methodology is the drop size distribution, and in our case, the 1-minute DSD measurements from the 2DVD can be utilized. However, the accuracy of small drops' concentration needs to be improved, which is possible by using data from one single camera alone for drop diameters below 0.5 mm. This will be attempted in the future.

7. Fall velocities

The 2DVD measurements for the aforementioned event in Huntsville had also indicated that the drop fall speeds may be affected by the mixed-mode oscillations within the organized line convection, in fact reducing the fall speeds for a significant fraction of the larger drops (say, D > 3 mm). There were two 2DVD instruments installed side-by-side, and in both cases, the time series of drop fall speeds showed that, during the period of the passage of the narrow convection line, considerable slowing down of the drops was seen for a significant fraction of the drops, compared to those measured after the time period (i.e. well after the convection line had crossed the 2DVD site).

The lower velocities observed in that event are somewhat consistent with the video images captured during the Mainz wind-tunnel experiments of drop collisions which show the larger drop to be slowing down during the transient period, until it reverts to the usual (2,0) mode. One example of the velocity measurements is shown in Fig. 6 for before, during and after collision, with the center of mass as being the reference. (Note the y-axis represents the vertical velocity, and is on a relative scale, which requires a scaling factor to be applied.) The drop collision occurs at around 360 msec after the start of the experiment. Prior to that, the drop vertical velocity is nearly zero. and upon collision, high fluctuations are seen. The time averaged variation (represented by the thick yellow line) shows an increase in the upward velocity for about 200 msec after collision, i.e. a lowering of the fall velocity. After several hundreds of milliseconds, the drop velocity reverts to its' near-zero values. Hence, it would seem that the collision-induced mixed-mode oscillation causes the fall velocity to temporarily reduce, then return to its normal (expected) velocity soon after the drop reverts to the (2,0) oscillation mode. This is a likely explanation for the lower fall velocity measurements from the 2DVDs for the Huntsville event during the passage of the narrow convection line, that is, it is quite possible that – at any given instant in time - sustained drop collisions can not only cause a significant fraction of drops to be in mixed-mode oscillations, but also to cause lower than the expected fall speeds, probably as a consequence of increased drag.

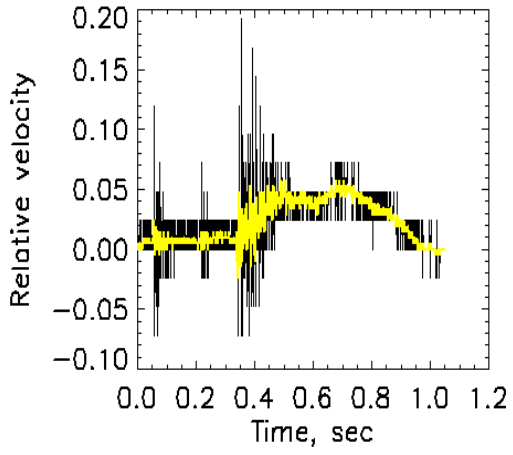

Fig. 6: Vertical velocity of the drop before, during, and after, collision.

8 Summary

Collision-induced drop oscillations have been investigated using an advanced vertical wind-tunnel facility. More than 130 cases were recorded with a high speed digital video camera. Many of the recorded collision events had to be abandoned because the drops were not in the focal plane of the camera. However, it was possible to analyze around 40 collision events. Among these were 27 which resulted in drop coalescence, and the remaining in non-coalescence collision. The sizes of the colliding drop pairs were chosen to be typical for real-atmospheric conditions, i.e. for the collector drops, they were in the 2.4 mm - 3 mm drop diameter range, while the small droplets had sizes of around 500 microns.

Data analysis clearly shows that the larger drop - upon collision - undergoes mixed-mode oscillations, with (2,1) and (2,2) modes dramatically increasing in oscillation amplitudes. The perturbation caused by the collision lasts for over several hundred milliseconds before effectively getting damped out and reverting to its usual (2,0) oscillation mode as the dominant mode. The coalescence cases show somewhat more pronounced mixed mode oscillations compared with the non-coalescence cases.

The drop vertical velocities of the larger drops were also calculated, with the center of mass as being the reference. A clear lowering of the fall velocity was indicated, the decrease lasting until after the drop reverts to the (2,0) oscillation mode.

These results have been discussed in conjunction with the previously reported 2DVD measurements during a widespread rain event with a narrow, embedded, line convection, where the 2DVD measurements had shown a lowering of fall velocities and a lack of rotational symmetry axis for a significant fraction of moderate-to-large drops during the passage of the line convection. In view of the wind-tunnel experiment results, a likely explanation is that sustained drop collisions within the narrow convection line cause a significant fraction of the drops to be in mixed mode oscillations at any given instant in time and that due to increased drag, the fall velocity of these drops is reduced. Such hypothesis will be tested in the future, as part of our ongoing investigations into drop shapes and fall velocities in natural rain.

Acknowledgements

The work is primarily supported by the National Science Foundation via grant AGS-0924622. We also wish to thank Simon Kessler for assistance with the experiments and to other colleagues associated with the wind-tunnel facility at Johannes Gutenberg University, Germany, for useful discussions.

References

Beard, K. V., 1976: Terminal velocity and shape of cloud and precipitation drops aloft. J. Atmos. Sci., 33, 851–864.

Beard, K. V., and R. J. Kubesh, 1991: Laboratory Measurements of Small Raindrop Distortion. Part 2: Oscillation Frequencies and Modes. J. Atmos. Sci., 48, 2245–2264.

Beard, K. V., V. N. Bringi, and M. Thurai, 2010: A new understanding of raindrop shape, Atmos. Res., 97, 396-415.

Bringi, V.N., and V. Chandrasekar, 2001: Polarimetric Doppler Weather Radar: Principles and Applications, Cambridge University Press, 636 pp.

Feng, J. Q., and K. V. Beard, 1991: A perturbation model of raindrop oscillation characteristics with aerodynamic effects. J. Atmos. Sci. 48, 1856–1868.

Jameson, A. R., and Durden, S. L., 1996, A possible origin of linear depolarization observed at vertical incidence in rain, J. Appl. Meteorol., vol. 35, 271-277.

Jameson, A. R., and A. B. Kostinski, 1999: Fluctuation Properties of Precipitation. Part V: Distribution of Rain Rates—Theory and Observations in Clustered Rain. J. Atmos. Sci., 56, 3920–3932

Johnson, D. B., and K. V. Beard, 1984: Oscillation Energies of Colliding Raindrops. J. Atmos. Sci., 41, 1235–1241.

McFarquhar, G. M., 2004: The effect of raindrop clustering on collision-induced break-up of raindrops, Q. J. R. Meteorol. Soc., 130, 2169–2190

Mitra, S. K., J. Brinkmann, and H. R. Pruppacher, 1992: A wind tunnel study on the drop-to-particle conversion. J. Aerosol Sci., 23, 245–256.

Pruppacher, H. R., 1988: Auswaschen von atmosphärischen Spurenstoffen durch Wolken und Niederschlag mittels eines vertikalen Windkanals. (Scavenging of trace gases by clouds and precipitation using a vertical wind tunnel.) Gesellschaft für Strahlen- und Umweltforschung, BPT-Bericht 9/88, 62 pp.

Rogers, R. R., 1989: Raindrop collision rates, J. Atmos. Sci. 46, 2469-2472.

Szakáll, M., K. Diehl, S. K. Mitra, and S. Borrmann, 2009: A Wind Tunnel Study on the Shape, Oscillation, and Internal Circulation of Large Raindrops with Sizes between 2.5 and 7.5 mm. J. Atmos. Sci., 66, 755–765.

Thurai, M., G. J. Huang, V. N. Bringi, W. L. Randeu, and M. Schönhuber, 2007: Drop Shapes, Model Comparisons, and Calculations of Polarimetric Radar Parameters in Rain. J. Atmos. Oceanic Technol., 24, 1019–1032.

Thurai, M., V. N. Bringi, M. Szakáll, S. K. Mitra, K. V. Beard, and S. Borrmann, 2009a: Drop Shapes and Axis Ratio Distributions: Comparison between 2D Video Disdrometer and Wind-Tunnel Measurements. J. Atmos. Oceanic Technol., 26, 1427–1432.

Thurai, M., V. N. Bringi, W. A. Petersen, and P. N. Gatlin, 2013: Drop shapes and fall speeds in rain: two contrasting examples, Journal of Applied Meteorology and Climatology, accepted for publication. Early on-line release.

Tokay, A. and K. V. Beard, 1996: A field study of raindrop oscillations. Part I: Observation of size spectra and evaluation of oscillation causes. J. Appl. Meteor., 35, 1671–1687.

Vohl, O., 1989: Die dynamischen Charakteristika des Mainzer vertikalen Windkanals. (The dynamic characteristics of the Mainz vertical wind tunnel.) M.S. thesis, Institute of Atmospheric Physics, Johannes Gutenberg University, 143 pp.